Journal of Sedimentary Research

Journal of Sedimentary Research, 2009, v. 79, 673–688
Research Article
DOI: 10.2110/jsr.2009.070

COMPENSATIONAL STACKING OF CHANNELIZED SEDIMENTARY DEPOSITS

KYLE M. STRAUB,*[1] CHRIS PAOLA,[1] DAVID MOHRIG,[2] MATTHEW A. WOLINSKY,†[1] AND TERRA GEORGE§[2]
[1]*Department of Geology and Geophysics, St Anthony Falls Laboratory, University of Minnesota, Minneapolis, Minnesota 55414, U.S.A.*
[2]*Department of Geological Sciences, The University of Texas at Austin, Austin, Texas 78712, U.S.A.*
e-mail: kmstraub@tulane.edu

ABSTRACT: **Compensational stacking, the tendency for sediment transport systems to preferentially fill topographic lows through deposition, is a concept widely used in the interpretation of the stratigraphic record. We propose a metric to quantify the degree of compensation by comparing observed stacking patterns in subsiding basins to what would be expected from uncorrelated random stacking. This method uses the rate of decay of spatial variability in sedimentation between picked depositional horizons with increasing vertical stratigraphic averaging distance. We present data from six sedimentary basins where this decay can be measured. The depositional environments range from river deltas to deep-water minibasins, and scales range from meters to 1.5 km in thickness. The decrease in standard deviation of sedimentation divided by subsidence with increasing vertical averaging distance is well described by a power law in each study basin. We term the exponent in this power law the *compensation index*, κ; its value is 0.5 for uncorrelated random stacking and 1.0 for perfect compensational stacking. Values less than 0.5 indicate anti-compensation, i.e., a tendency of depositional units to stack on top of one another. Parameters controlling the magnitude of κ include the frequency of system-scale avulsions and the temporal variability in deposition rates. Data describing the decay in the standard deviation of sedimentation/subsidence from the six studied basins collapse approximately onto a single power-law trend with $\kappa = 0.75$ when the measurement window is standardized by the mean channel depth of each system. Channel depth thus emerges as a fundamental length scale in stratigraphic architecture across environments. Although further study will likely reveal measurable variability in κ between depositional environments, the overall power-law collapse presented here suggests that a stacking behavior midway between purely random and perfect compensation is a good starting point in quantitatively estimating the stratigraphic arrangement of sedimentary deposits.**

INTRODUCTION

When sedimentary deposits are constructed by discrete elements such as channels and lobes, morphodynamics combines with subsidence to create a characteristic depositional "architecture" that controls the three-dimensional (3D) structure of the strata. This architecture is strongly influenced by the degree to which the positions of recent depositional elements are influenced by the locations of previous elements. For example, in the original fluvial architecture model of Leeder (1978) the channel positions are assumed to be random and independent of previous channel locations. In contrast, in a later model Allen (1979) proposed that abandoned channels would remain high for a time, leading to avoidance of previous channels and an overall tendency to distribute channel bodies more evenly than in Leeder's model. Jerolmack and Paola (2007) developed a cellular channel model in which relict channels served as attractors until they were filled with sediment, leading to development of multi-story channel bodies.

The channel "avoidance" model can be generalized to other kinds of depositional elements, like lobes, and is widely used in interpreting the stratigraphic record. Sedimentary deposits arranged in this manner are often referred to as being the product of *compensational stacking*. Here we use experiments on fluvial systems in basins experiencing relative subsidence together with industry-grade 3D seismic data from deep marine and fluvial delta settings to quantify compensational stacking. Our overall strategy is to develop a practical, readily applicable measure for the degree of compensation by comparing observed stacking patterns to what would be expected from simple, uncorrelated random stacking.

Compensational stacking describes the tendency of flow-event deposits to preferentially fill topographic lows, smoothing out topographic relief "compensating" for the localization of deposition by discrete depositional elements. This tendency is thought to result from either a continuous or a periodic reorganization of the sediment transport field to minimize potential energy associated with elevation gradients (Mutti and Normark 1987; Stow and Johansson 2000). The initial compensational stacking models were developed to describe the formation of thick tabular deposits of amalgamated turbidites from individual depositional units that are distinctly nonplanar in form. More recently, compensational stacking has been used to describe the large-scale architecture of fluvial deposits, in particular delta packages (Olariu and Bhattacharya 2006; van Wagoner 1995). Examples of stratigraphic architectures typically interpreted as being constructed by compensational stacking are shown in Figure 1. Early models by Mutti and Sonnino (1981) and Mutti and Normark (1987) describe depositional cycles resulting from compensational stacking. In these models the structure of the submarine sediment-

* Present Address: Department of Earth and Environmental Sciences, Tulane University, New Orleans, Louisiana 70118, U.S.A.
† Present Address: Shell International Exploration and Production, Inc., Houston, Texas 77001, U.S.A.
§ Present Address: ConocoPhillips Company, Houston, Texas 77079, U.S.A.

 1527-1404/09/079-673/$03.00

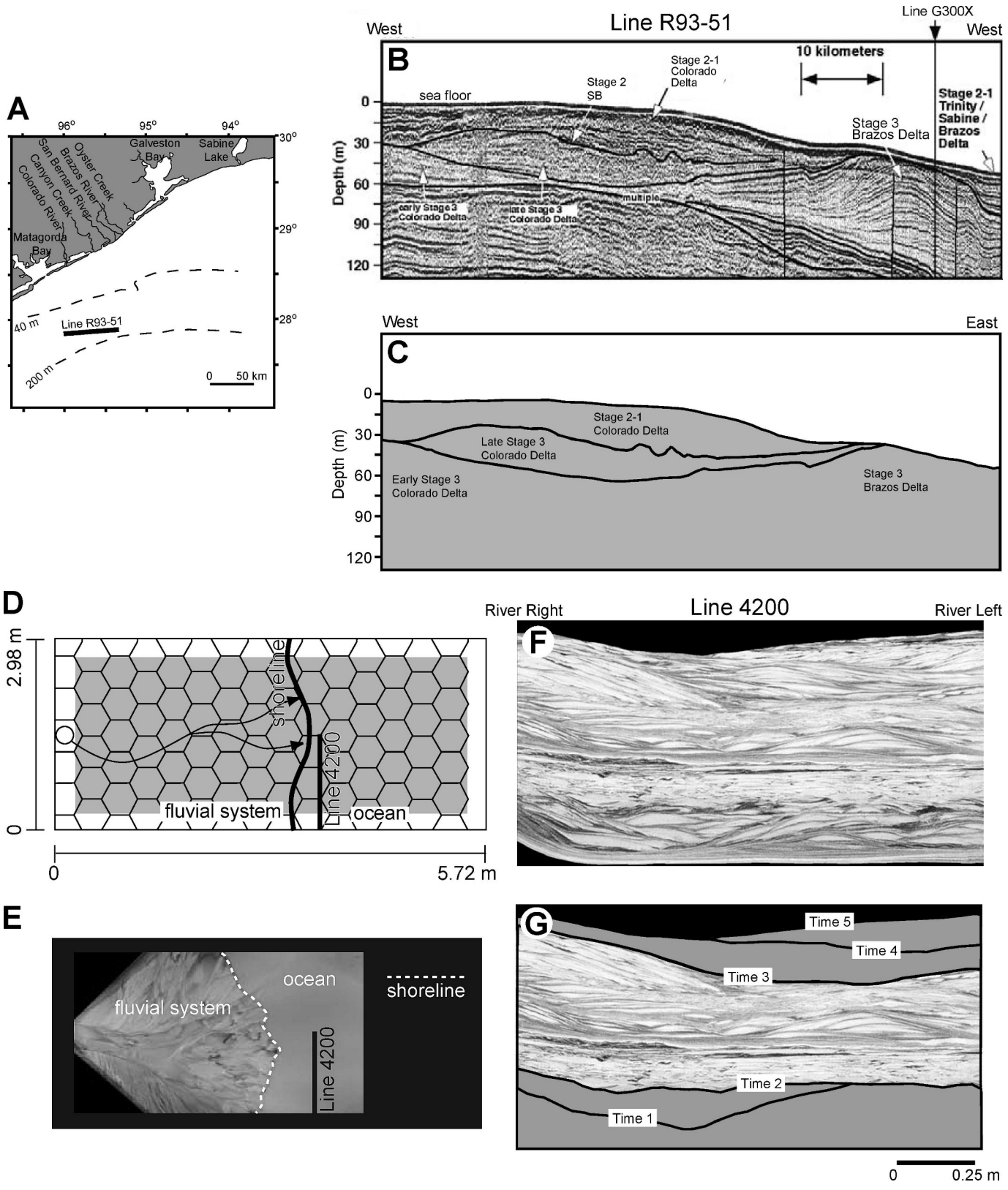

FIG. 1.—Examples of stratigraphic architectures that could be interpreted as compensational stacking. **A–C)** Stratigraphy of the upper 120 m of the continental shelf offshore Texas in the Gulf of Mexico (Anderson et al. 2004). Shelf-edge parallel seismic cross section reveals paleo-topographic low which existed between the Early Stage 3 Colorado River Stage 3 Brazos River deltas. This low is filled in during the construction of the Late Stage 3 and Stage 2–1 Colorado River deltas. This stacking pattern smoothes topography and thus could be termed compensational. Images reproduced with the permission of SEPM. **D–G)** Stratigraphy generated in the Experimental EarthScape (XES) basin during an experiment investigating the control of baselevel fluctuations on stratigraphic architecture. See Martin (2007) and Kim et al. (2006) for

transport field remains fixed over short time intervals, resulting in lenticular deposits with positive surface relief. Periodic channel or lobe avulsion then occurs, reorganizing the sediment transport field along local topographic lows. The sediment transport field then remains approximately fixed in space and the bed aggrades via a focusing in sediment deposition until sufficient surface topography develops to drive a new avulsion.

Recent field studies have documented bedding structures that are believed to result from compensational stacking below the channel and lobe scale described by Mutti and Sonnino (1981). Stow and Johansson (2000) and Deptuck et al. (2008) show that small-scale geometries commonly mimic the large-scale channel and lobe geometries so that a lobe itself may be constructed of compensationally stacked depositional elements. Recently developed stochastic surface-based models of turbidite lobes (Pyrcz et al. 2005) incorporate compensational stacking. While a wealth of field and subsurface observations support organization of stratigraphic deposits by compensational stacking (Hodgson et al. 2006; Johnson et al. 2001; Mitchum and Van Wagoner 1991; Satur et al. 2000) a quantitative metric has yet to be developed to measure the strength of this tendency. Our aim here is to provide such a metric.

One key question that has not been addressed to date is how to separate depositional patterns that specifically result from topographically driven compensation from depositional patterns that are arranged randomly. This difficulty exists because deposits resulting from the latter scenario occasionally, but not always, occur in topographic lows and thus appear to be driven by compensation. As a result, qualitatively separating random and topographically driven processes is challenging, (Note that by "random" we mean probabilistic processes that have no detectable correlation in space or time; we use "stochastic" as a general term for probabilistic processes regardless of correlation.) In this manuscript we build on methods developed to asses the balance between sedimentation and subsidence by Sheets et al. (2002) and Lyons (2004) to develop a statistical compensation index to measure the tendency of marine and terrestrial depositional systems to fill basins through compensational stacking. Using the compensation index, we then compare observed stacking patterns in sedimentary basins to stochastic stacking models in which we can vary the degree of correlation systematically.

Sheets et al. (2002) studied the transition in alluvial depositional geometry from morphologies controlled by local channel geometry to morphologies controlled by regional sediment supply and accommodation. This study was based on depositional patterns developed in the Experimental EarthScape (XES) facility (Paola et al. 2001). The interval needed for this transition from short-term (flow-controlled) to long-term (subsidence-controlled) depositional geometry was measured in terms of vertical deposit thickness in the XES-99 experiment. Sheets et al. (2002) proposed that the deposit thickness (i.e., time) required to make this transition could be scaled to the time needed for channels to visit every spot in the basin repeatedly, averaging out local autogenic effects and bringing the geometry of the long time scale depositional package into balance with the accommodation. This time interval is called the *stratigraphic integral scale*. Sheets et al. (2002) found that the stratigraphic integral scale was equal to the time required to aggrade the bed by a vertical distance equal to about seven channel depths, regardless of the subsidence rate. Methods developed by Lyons (2004) allow the stratigraphic integral scale to be measured for natural systems. Below we outline the methods for calculating the stratigraphic integral scale for experimental and field settings; then we apply these methods to observations from Sheets et al. (2002), Lyons (2004), and two additional basins. By analyzing limiting cases of random stacking versus perfect compensation, we then establish a generalized compensational stacking framework in which the degree of compensation and its effects on stratal architecture can be measured and quantified.

THE STRATIGRAPHIC INTEGRAL SCALE

A stratigraphic integral scale can be defined in any sedimentary basin where over some length scale the long-term supply of sediment is roughly in balance with subsidence. Sheets et al. (2002) developed a method for estimating the stratigraphic integral scale for basins in which subsidence and sedimentation histories are known for short time spans (flow-controlled) and long time spans (subsidence-controlled). This method is based on the ratio of sedimentation to subsidence measured over these varying time spans. For simplicity, we begin with the case in which steady subsidence is the only external forcing, i.e., sea level, sediment supply, etc. remain constant, so that on long time scales the basin tends to a steady state in which sedimentation balances subsidence.

Over sufficiently long time intervals the sediment transport system has time to visit every spot in a basin repeatedly, and as a result the ratio of the local sedimentation rate to subsidence at any point in the basin should approach unity (Fig. 2). Over short time intervals, however, depositional geometries within a basin are controlled by the configuration of the transport system. As a result, the ratio of sedimentation to subsidence at any one point within the basin is highly variable. As the time scale of averaging increases, this variability diminishes. We define the standard deviation of sedimentation/subsidence (σ_{ss}) as

$$\sigma_{ss}(T) = \left(\int_A \left[\frac{r(T;\, x, y)}{\hat{r}(x, y)} - 1 \right]^2 dA \right)^{1/2} \tag{1}$$

where $r(T;\ x,\ y)$ is the local sedimentation rate measured over a stratigraphic time difference T (i.e., stratal thickness between two chronostratigraphic markers T apart, divided by T), x and y are horizontal coordinates, A is area measured parallel to stratal surfaces, and $\hat{r}$ is the long-term average sedimentation rate. The value of σ_{ss} serves as a measure of the extent of subsidence control in a basin. It approaches zero for time intervals over which subsidence balances deposition.

Sheets et al. (2002) tested their method for quantifying a stratigraphic integral scale in the XES basin, where subsidence rate and pattern can be controlled while continuously introducing sediment to the basin. To compare the (known and steady) subsidence rates with data on deposition rates, they measured the topography that developed in the basin at discrete time intervals. Sheets et al. (2002) presented results from three stages of that experiment. During stages 1 and 2, the depositional controls were essentially the same. In Stage 1, a cross-stream variation in subsidence rate was imposed in contrast to Stage 2 in which subsidence varied only in the streamwise direction. Stage 3 used the same spatial pattern as Stage 2 but rates of subsidence, along with water and sediment influx, were reduced to 25% of their Stage 2 values. For each measurement window in their experiment they divided a map of deposit thickness point wise by the net deposit thickness expected from subsidence alone for that time interval. They then calculated σ_{ss} as defined above and used this metric as a measure of the misfit between the two maps. Sheets and his colleagues plotted the decay of the standard deviation of sedimentation/subsidence against measurement time win-

←

more details on experiment. Interpretations of five time surfaces are shown in panel G from a strike-oriented stratigraphic section. Deposition that occurred between times 1 and 2 in addition to deposition that occurred between times 3 and 5 fills topographic lows and thus smoothes topography. This stacking pattern could be termed compensational.

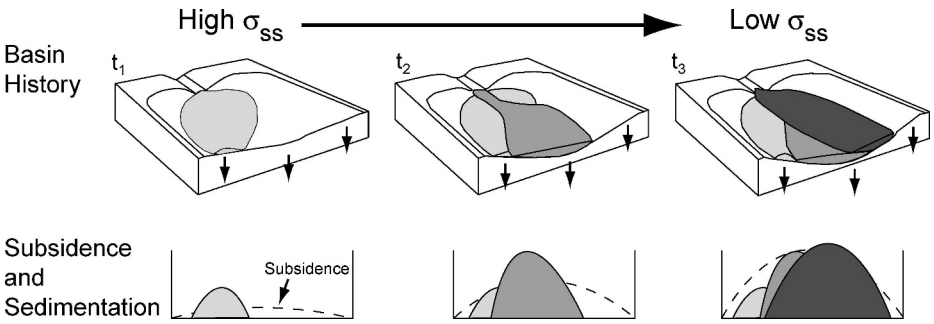

FIG. 2.—Schematic from Lyons (2004) describing the progression of a basin towards equilibrium. The balance between sedimentation and subsidence in a basin improves over time. In the block diagrams illustrating basin history, subsidence (indicated by arrows) is temporally constant but spatially variable. Sedimentation, represented by lobes of different color, is both temporally and spatially variable. The balance between sedimentation and subsidence for an arbitrary cross section at the three time steps is represented graphically below each block. At the earliest time, t_1, subsidence is small and sedimentation is local resulting in a poor fit between the two. However, as the basin develops, subsidence increases and the sedimentary system has an opportunity to occupy a larger fraction of the total area. The result then, at later times t_2 and t_3, is that the fit between sedimentation and subsidence improves. Taking the ratio of sedimentation over subsidence pointwise across the basin for each time step would produce ratio distributions with decreasing standard deviations over time.

dow, σ_{ss} vs. T, for each of their three stages and fitted the data with an exponential curve (Fig. 3A). The time constant from the fitted exponential provides a quantitative measure of the stratigraphic integral scale, allowing comparison of the different stages of their experiment.

Motivated by the experimental results of Sheets et al. (2002), Lyons (2004) developed a scheme to estimate the stratigraphic integral scale for field scale basins. This was done for the Fisk Basin in the Gulf of Mexico (GOM). The Fisk Basin is one of many mini-basins on the continental slope of the GOM formed as a result of salt diapirism (Salvador 1991). The basin is a site of active turbidity-current deposition (Winker and Booth 2000). Using a seismic volume that covers Fisk Basin, Lyons mapped six laterally persistent stratigraphic horizons within a 350 m thick section. With a time-depth curve that translates seismic time to depth below seafloor and biostratigraphic dates of stratigraphic horizons, Lyons was able to estimate sediment deposition rates in the basin over 16 measurement time windows. Deposition rates over these 16 time windows were restored to near-seafloor conditions by adjusting for the reduction in porosity due to post depositional compaction. Decompaction factors were determined from porosity vs. depth trends measured within the study region. Subsidence rates were measured for the basin using a number of biostratigraphic age dates that could be tied to specific seismic horizons, with the result that subsidence rates were roughly constant over the analyzed section.

Calculation of an integral time scale for the Fisk Basin required several assumptions regarding the shape and rate of subsidence in the basin, the most important of which was that the deposition pattern of the thickest stratigraphic interval mapped in the basin (350 m) was in balance with the average subsidence pattern. Lyons then estimated the magnitude of subsidence in the Fisk basin for a given stratigraphic window i as

$$S_{Dim} = S_{Norm} r_i T_i \tag{2}$$

where S_{Norm} is a normalized subsidence map, r_i is the mean deposition rate in the basin, and T_i is the amount of time contained within a stratigraphic window. S_{Norm} is taken to be the deposition map of the thickest stratigraphic interval divided by the maximum thickness in that window. Lyons then used maps of deposit thickness and subsidence to calculate σ_{ss} for the 16 stratigraphic windows constituting the section of stratigraphy studied. Similar to the results of Sheets et al. (2002), Lyons observed a decay in σ_{ss} as a function of T (Fig. 4A). This decay was then fitted with an exponential curve to estimate the e-folding time or stratigraphic integral scale.

QUANTIFYING COMPENSATIONAL STACKING

The methods developed by Sheets et al. (2002) and Lyons (2004) yield a quantitative metric for estimating the amount of time required to transition from deposit geometries dictated by the flow field to deposit geometries set by subsidence. While neither Sheets et al. (2002) nor Lyons (2004) comment on the influence of compensation as it relates to the time required to approach subsidence-controlled deposit geometries, their data can be used to examine this problem. To illustrate how plots of σ_{ss} against T can be used to measure the tendency of deposits to stack via compensation, it is first helpful to examine how σ_{ss} decays when stacking deposits of random thickness in a basin that is subsiding at a constant rate. This scenario represents construction of stratigraphy with no tendency for compensational stacking. A basic theorem from statistics holds that the sample mean of N independent random deviates converges to the population mean, with the standard error of the sample mean decaying as $N^{-1/2}$. Applied to the stratigraphic case, this implies that sedimentation rates measured over increasing interval thickness H should converge to the mean sedimentation rate as $H^{-1/2}$ if the increments of sedimentation are independent of one another. This would be the case with no compensation.

To realize this reference condition numerically, we construct one-dimensional (1D) stratigraphic columns composed of discrete beds where the thickness increment, $d\eta$, of each bed is chosen at random from a Gaussian distribution of thicknesses with a constant mean, $d\bar{\eta}$. In this model each bed represents the same amount of time, T_G, and the column subsides at a rate equal to $d\bar{\eta}/T_G$. We construct a large number of independent stratigraphic columns using this method (i.e., $n > 100{,}000$) with constant values of T_G and $d\bar{\eta}$ for each column. We then calculate σ_{ss} for the entire basin and plot this against measurement time window T. The results are shown in Figure 5. As expected σ_{ss} decays as a power-law function of measurement time window,

$$\sigma_{ss} = aT^{-\kappa} \tag{3}$$

where a and κ are respectively the coefficient and the exponent in the power law. For the current scenario with uncorrelated deposition increments, κ is equal to 0.5. Compensation, however, implies correlation in the depositional increments–in particular, compensation requires a negative correlation in increment thickness, because depositional increments thinner than the mean value must on average be followed by (compensated by) relatively thick increments. We show next that any

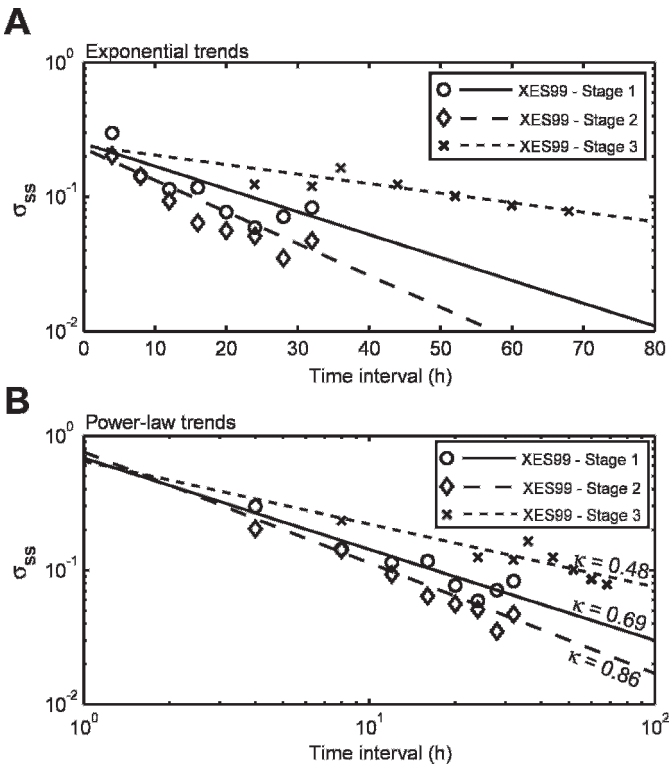

FIG. 3.—Decay of σ_{ss} with increasing time interval for three experimental stages of XES99 experiment from Sheets et al. (2002). Data from stages are fit with both **A)** exponential trend lines and **B)** power-law trend lines.

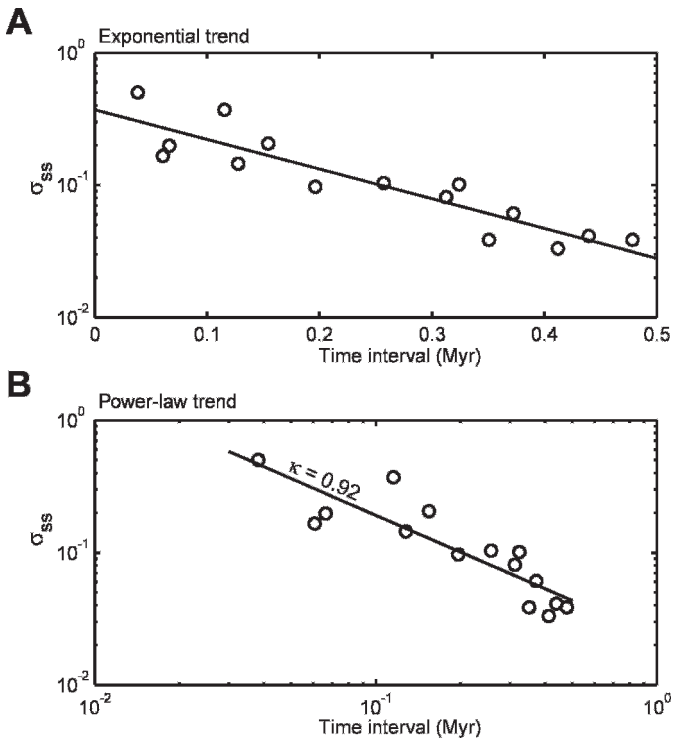

FIG. 4.—Decay of σ_{ss} with increasing time interval for Fisk Basin channelized stratigraphy presented in Lyons (2004). Data are fitted with both **A)** exponential trend line and **B)** power-law trend line.

such correlation in the deposition process is reflected in changes in κ away from the reference value of 0.5. Hence we term κ the *compensation index*.

As a next step in our analysis of σ_{ss} we artificially add compensation to our 1D stratigraphic columns. This is done through a lag-one autoregression, or Markov scheme:

$$d\eta_t = \phi d\eta_{t-1} + d\eta \tag{4}$$

where φ is a constant that represents the degree of correlation of the sedimentation increments (i.e., the strength of compensation) in the system and $d\eta$ is chosen at random for each time step in a manner similar to the 1D model described above. 1D stratigraphic models that incorporate various degrees of persistence in sedimentation trends have previously been used to examine bed statistics (Pelletier and Turcotte 1997). When $\varphi = 0$, Equation 4 reduces to the uncorrelated scenario above and thus yields a power law with $\kappa = 0.5$. However, when φ is negative Equation 4 produces 1D compensation: the deposition of a thin bed during one time step is statistically more likely to be followed by a thick bed in the succeeding time step, and vice versa. In this model $\varphi = -1.0$ produces pure compensational stacking of deposits and yields $\kappa = 1.0$. When $\varphi > 0$, Equation 4 produces stratigraphic persistence, or what in the present context might be termed "anti-compensation": a thin bed during one time step is statistically more likely to be followed by a thin bed in the succeeding time step, and vice versa, resulting in φ values less than 0.5. In the case where $\varphi = 1.0$, $\kappa = 0.0$.

These 1D models suggest that the tendency of deposits to stack compensationally can be measured through the decay of σ_{ss} with time. Specifically, they suggest that the decay of σ_{ss} for natural basins should follow a power law and have compensation index (κ) values between 0 and 1.0, with these end-member values representing perfect persistence (anti-compensation) that tends to amplify depositional topography and perfect compensation, respectively. The end member $\kappa = 0$ is unlikely to occur in nature, but some degree of persistence is certainly possible, as indicated for example by multi story channel sand bodies (e.g., Jerolmack and Paola 2007). However, our focus here is on the range of κ values between 0.5 and 1.0, i.e., between purely random stacking and perfect compensation.

These findings prompt two questions: (1) does the decay of σ_{ss} in natural basins follow power-law relationships, and if so (2) what is the range of κ values for natural basins?

COMPARISON WITH FIELD AND EXPERIMENTAL DATA

To answer these questions we start by reanalyzing data presented by Sheets et al. (2002) and Lyons (2004). In these studies the decay of σ_{ss} was modeled using an exponential decay with measurement time. However, in both studies, reported values of σ_{ss} at small measurement time windows were underestimated by exponential least-squares fits. Lyons (2004) assumed that the observed divergence was due to small-scale mapping errors of interpreted horizons that strongly influence the value of σ_{ss} for small measurement time windows. We refit the data sets of Sheets et al. (2002) (Fig. 3B) and Lyons (2004) (Fig. 4B) with power-law trends and compare the quality of exponential vs. power-law fits by way of the regression R^2 values. The R^2 values of power-law and exponential fits were similar for all four data sets; however, the Fisk Basin data, in addition to the first two of the three stages of the XES experiment, are slightly better described by power-law relationships (Table 1). Visual inspection shows that power-law trends improve the quality of the fits for small measurement time windows. The values of κ in the power law fits vary between 0.5 and 0.9 for the four data sets.

To determine if the decay of σ_{ss} in sedimentary basins is best described by a power-law trend, and to examine how this trend varies in different settings, we next present data describing how σ_{ss} varies with measurement time window for two additional data sets. First we present high-temporal-

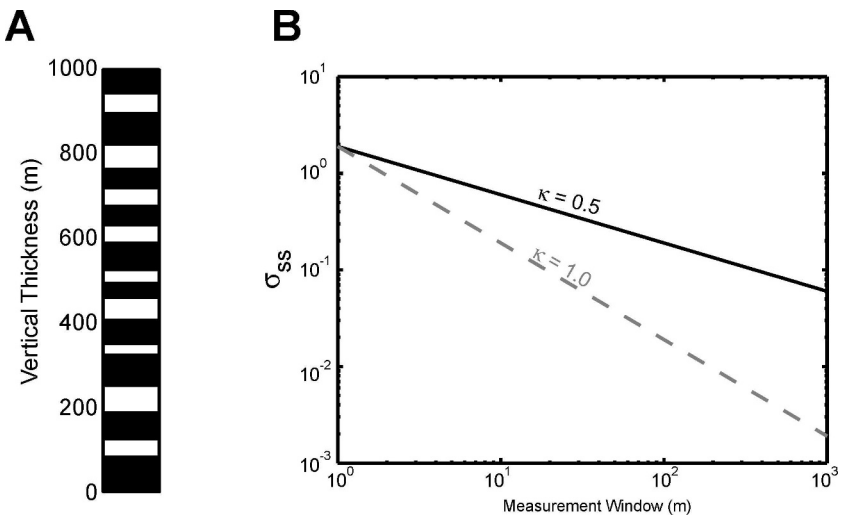

FIG. 5.—Illustration of 1D model used to examine the decay of σ_{ss} with measurement window for stratigraphic columns built from beds with Gaussian distribution of bed sizes. We construct a large number ($n > 100{,}000$) of stratigraphic columns where individual beds in the column are randomly picked from a Gaussian distribution with an assigned mean and standard deviation. Subsidence associated with any stratigraphic window is assumed to equal the mean bed deposit thickness multiplied by the number of beds. **A)** A sample stratigraphic column constructed from a Gaussian distribution with a mean bed thickness of 50 m and a standard deviation of 20 m. **B)** This distribution in bed sizes produces a power law decay of σ_{ss} with a κ equal to 0.5 (solid black line). When pure compensation is added to the random model through a Markov scheme, the power-law decay is associated with a κ value of 1.0 (dashed gray line).

resolution data on the decay of σ_{ss} for a delta in an experimental basin with aggradation driven by relative rise in base level. This data set allows us to examine if the decay of σ_{ss} follows a power-law or an exponential trend. Second, we utilize an industry-grade 3D seismic survey from the Mississippi delta top to measure the decay of σ_{ss} in a terrestrial field-scale basin. This second data set allows us to compare the decay of σ_{ss} in terrestrial and submarine environments in addition to laboratory-scale and field-scale basins.

High-Temporal-Resolution Experimental Stratigraphy

Results documenting the evolution of stratigraphy in the XES-99 experiment constrain the stratigraphic integral scale for the basin under three subsidence/sediment-transport scenarios. We found that power-law and exponential trends fit these data with approximately equal accuracy over the time windows provided by the mapping frequency in the experiment. These trends, however, deviate significantly from one another for measurement time windows below the mapping frequency. To determine if the decay of σ_{ss} with measurement time follows a power-law or an exponential trend we analyze data from an experimental basin in which stratigraphy developed under a subsidence/sediment-transport scenario similar to the second stage of the XES-99 experiment: in this experiment, DB-03, topography was measured at a sampling frequency 120 times greater than in the XES-99 experiment.

The DB-03 experiment was performed in the Delta Basin at St. Anthony Falls Laboratory at the University of Minnesota. This basin is 5 m by 5 m and 0.61 m deep (Fig. 6). Accommodation is created by slowly increasing base level using a siphon-based controller that controls base level with millimeter-scale resolution (Sheets et al. 2007). The experiment included an initial buildout phase in which sediment and water were mixed in a funnel and fed into one corner of the basin while base-level remained constant. The delta was allowed to prograde into the basin and produced an approximately radially symmetrical fluvial system. After the system prograded 2.5 m from source to shoreline, base-level rise was initiated at a rate equal to the total sediment discharge (Qs) divided by the desired delta-top area. This sediment feed rate allowed the shoreline to be maintained at an approximately constant location through the course of the experiment. The experimental deposit, including the topographic measurement lines, is shown in Figure 7. Sheets et al. (2007) used a sediment mixture of 70% 120 μm silica sand and 30% bimodal (190 μm and 460 μm) anthracite coal. A comparison of the experimental parameters of this experiment and stage 2 of XES-99 is presented in Table 2.

TABLE 1.—*Comparison of exponential and power-law trend-line fits for the six data sets in this study.*

System	Exponential R^2	Power-law R^2	κ
XES99 - Stage 1	0.71	0.88	0.69
XES99 - Stage 2	0.91	0.96	0.86
XES99 - Stage 3	0.82	0.81	0.49
Fisk Basin	0.83	0.78	0.92
DB03	0.81	0.98	0.81
Breton Sound	0.89	0.93	0.71

Topographic measurements were taken in a manner modeled on the XES subaerial laser topography-scanning system (Sheets et al. 2002). Unlike the XES-99 experiment, in which the topography of the entire fluvial surface was recorded periodically, DB-03 topography was monitored at 2 minute intervals along three flow-perpendicular transects, located 1.50 m, 1.75 m, and 2.00 m from the infeed point. This arrangement allowed for extremely rapid collection of topographic measurements, rather than the 30 to 45 minutes required for a full-surface scan. The DB-03 system records topography every 0.8 mm along transects with a vertical resolution of 0.9 mm. A time series of deposition along the 1.75 m transect is shown in Figure 8. This experiment lasted for 30 hours and produced an average of 0.20 m of stratigraphy.

Similarly to the XES-99 experiment, we calculated the ratio of sedimentation to subsidence at each measurement location for every possible pairwise combination of topographic surveys. The standard deviation σ_{ss} of sedimentation relative to subsidence was then calculated for all data points that share the same run-time interval between differenced topographic surveys. This allows us to define the decay of σ_{ss} over measurement windows of 2–1800 minutes (Fig. 9), a range approximately one order of magnitude greater than available for stage 2 of XES-99. Next we calculated the stratigraphic integral scale (from an exponential trend line) and κ (from a power-law trend line) for the experiment. The stratigraphic integral scale was 11 hours compared to 17 hours for stage 2 of XES-99, while κ was 0.81 compared to 0.86 for stage 2 of XES-99. We compared power-law and exponential regressions via trend R^2 values, similar to the comparison performed on data from XES-99 and the Fisk Basin (Table 1). We found that an exponential data fit produced an R^2 value of 0.81 compared to 0.98 for the power-law fit.

Mississippi Delta

The Mississippi Delta is a large river-dominated delta as classified by Galloway and Hobday (1996) that has been the focus of many

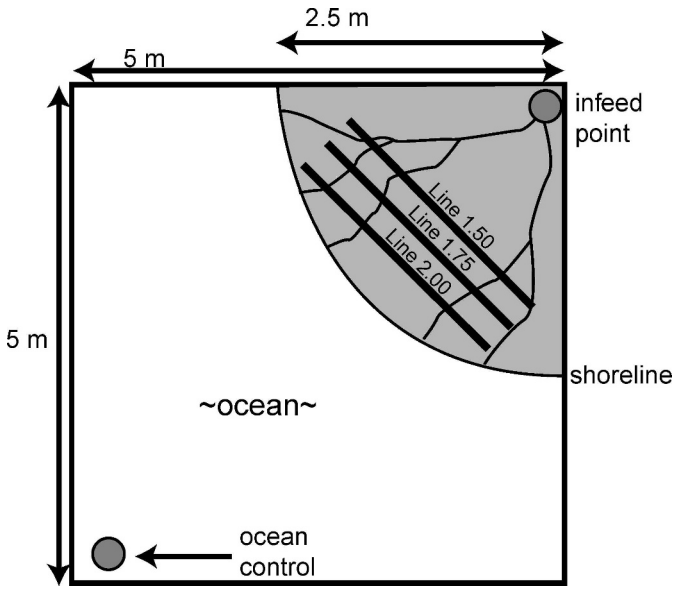

FIG. 6.—Schematic diagram of the Delta Basin facility and DB03 experiment. Positions of the topographic transects are indicated by solid black lines on the fluvial surface. Note that the base-level-control drain is in the opposite corner of the basin from the infeed point.

sedimentology studies over the last century due to its social, economic, and environmental importance (Morton et al. 2003; Van Beek and Meyer-Arendt 1982). Many of these studies have focused on the stratigraphy of the Mississippi Delta as it relates to petroleum exploration (Galloway et al. 2000; Weimer 1990). Of particular importance to this study is a subset of data collected by the petroleum industry that includes 3D seismic data.

Sediment deposition from the Mississippi River has constructed up to 15 vertical km of stratigraphy beneath its present-day delta (Salvador 1991). Creation of long-term accommodation space in the lower Mississippi basin has been achieved through flexure of the GOM lithosphere in response to sediment loading, cooling of oceanic crust, withdrawal of mobile salt, and active growth faulting along the delta front (Galloway et al. 2000; Salvador 1991; Schuster 1995). The availability of 3D seismic data over large sections of this subsidence-sedimentation environment make it a superb site to quantify the decay of σ_{ss} in a field-scale terrestrial setting.

Here we focus on the sedimentation and subsidence history of the Mississippi Delta below 800 km^2 of Breton Sound (Fig. 10) located approximately 100 km southeast of New Orleans, Louisiana. Breton Sound is a shallow embayment of the Gulf of Mexico, average water depth 5 m, situated directly east of the present-day Mississippi River on the delta topset. Our study uses an industry-grade 3D seismic survey that images the upper 1.2 km of Mississippi Delta stratigraphy and was made available by WesternGeco, Inc. The frequency roll-off for the seismic volume is near 40 Hz, providing a vertical resolution of ~ 10 m. The entire survey was collected on a horizontal grid with 110 ft (~ 35.6 m) spacing.

A high-resolution chronology for the stratigraphy in this region of the Mississippi Delta has yet to be constructed. Fortunately, paleontological data from a petroleum well located 39 km to the west of our study area is publicly available and yields an estimated long term subsidence rate of 0.26 m/kyr (Fig. 11). This value is similar to the regional long-term subsidence rates (10 kyr–10 Myr) estimated by Fillon (2004 and references therein).

Stratigraphic horizons mapped within the 3D reflection seismic volume were converted from two-way travel time (TWT) to true depth using data

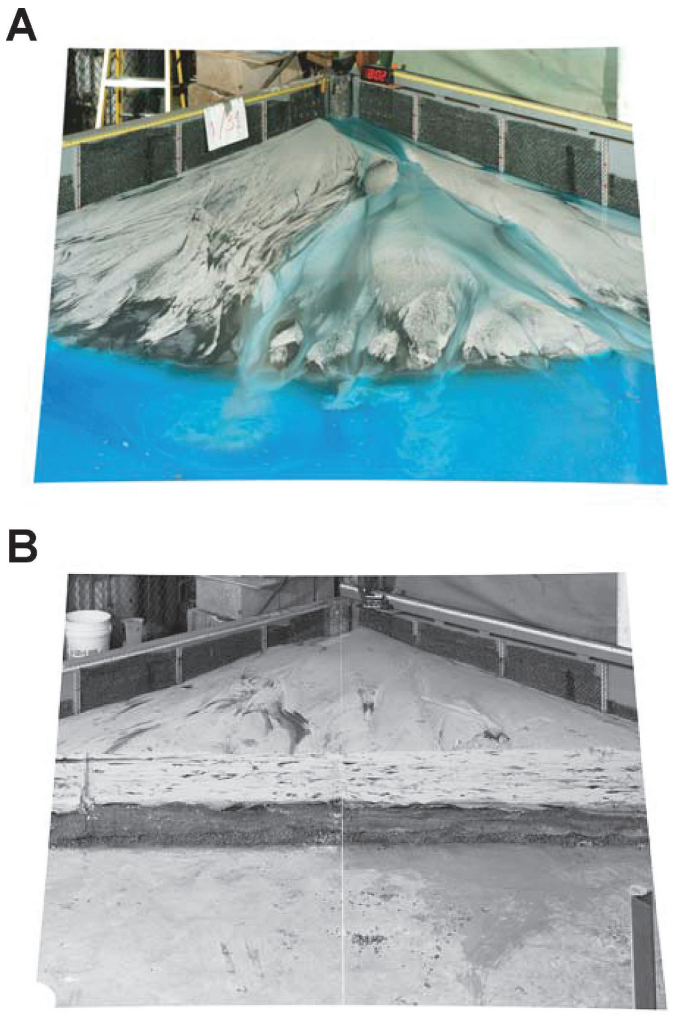

FIG. 7.— Photographs of DB03 experiment. **A)** Photograph taken approximately 15.0 hr into the DB03 experiment. System is approximately 2.5 m in length from source (back center) to shoreline. Topographic measurements were taken along the three laser sheet lines seen in the photograph. **B)** Photograph of approximately 0.2 m of stratigraphy generated during DB03 experiment. Stratigraphic section is located at approximately 1.75 m from source.

from five borehole-derived check-shot surveys (Fig. 12). These surveys were collected by four different operators from wellbores located within our study region. We fit time–depth pairs from these surveys with a polynomial to construct the following conversion function:

$$D = 141.8\ \mathrm{m/s^2}\left(TWT_{sh}^2\right) + 818.9\ \mathrm{m/s}\left(TWT_{sh}\right) \quad (5)$$

where D is vertical distance beneath the seafloor in meters and TWT_{sh} is the two-way travel time at the subsurface position of interest. Equation 5 is applied locally to convert grids of points defining horizons in two-way travel time to grids of points defining the same horizon in depth below the seafloor.

We used the Breton Sound seismic volume to map nine seismic horizons in the upper 1.2 km of stratigraphy. The horizons have been named MD1 through MD9 with increasing depth below the present-day seafloor (Fig. 13). These seismic horizons were selected for mapping because they have strong reflection amplitudes that can be tracked over the full extent of the seismic volume. The seismic horizons were picked on each in-line of the seismic volume, thus creating the highest-resolution maps possible with this data set. The fact that these seismic horizons can

TABLE 2.—*Comparison of experimental parameters between DB-03 and XES99 stage 2.*

Experiment	Q_w (Ls^{-1})	Q_s (Ls^{-1})	Q_w:Q_s	Avg. Aggradation rate (mm/hr)	Avg. Slope
DB 03-1	0.4	0.01	40:1	5.0	0.05
XES 99 (stage 2)	0.53	0.0136	39:1	7.0	0.047

be traced throughout the entire study region suggests that they represent condensed sections of fine-grained material deposited during relative highstands in sea level. Maps of the nine subsurface seismic horizons are approximate realizations of paleo-topography. When analyzed in conjunction with the present-day bathymetry in our study region, they allow us to evaluate how the balance of sediment deposition and subsidence changes as a function of mean stratigraphic unit thickness.

We measured the decay of σ_{ss} for the upper 1.2 km of stratigraphy in our study region using a modified version of the methods developed by Lyons (2004). The first step in this process is to create maps of stratigraphic thickness by differencing all possible pairwise combinations of depth-converted seismic horizons. Using the nine seismic horizon maps in addition to the present-day seafloor, this process resulted in the creation of 44 stratigraphic thickness maps. Once stratigraphic thickness maps are generated, a correction is applied so that each map approximates near-seafloor deposit thickness. This correction accounts for a reduction in porosity due to post depositional compaction and thus a reduction in deposit thickness with burial. In order to convert our stratigraphic thickness maps to near-seafloor thickness maps we first estimated how porosity varies with depth in our study region. This trend is estimated using the Raymer–Hunt–Gardner (Raymer et al. 1980) method to transform interval sonic transit times to porosities. Applying this method to data from the five check-shot surveys produces a nearly linear reduction in porosity from 48% at the seafloor to 38% at 1.5 km depth. The inflation of the 44 stratigraphic thickness maps to near-seafloor conditions resulted in deposits that ranged from 24 to 1389 m in mean thickness. Figure 14 shows a subset of these thickness maps. For thin stratigraphic intervals, 20–200 m of average aggradation, there is significant variability in the spatial pattern of deposition. However, at stratigraphic intervals with mean aggradation of 200–600 m, the variability in deposition pattern decreases. Further, the pattern of deposition between the top half of the stratigraphic section analyzed (MD5-seafloor) and the lower half (MD9–MD5) appears similar in map view. Following Lyons (2004), we take the reproducibility of the depositional pattern at "intermediate" stratigraphic intervals as evidence for an invariant subsidence pattern throughout the time interval associated with the total stratigraphic interval of interest.

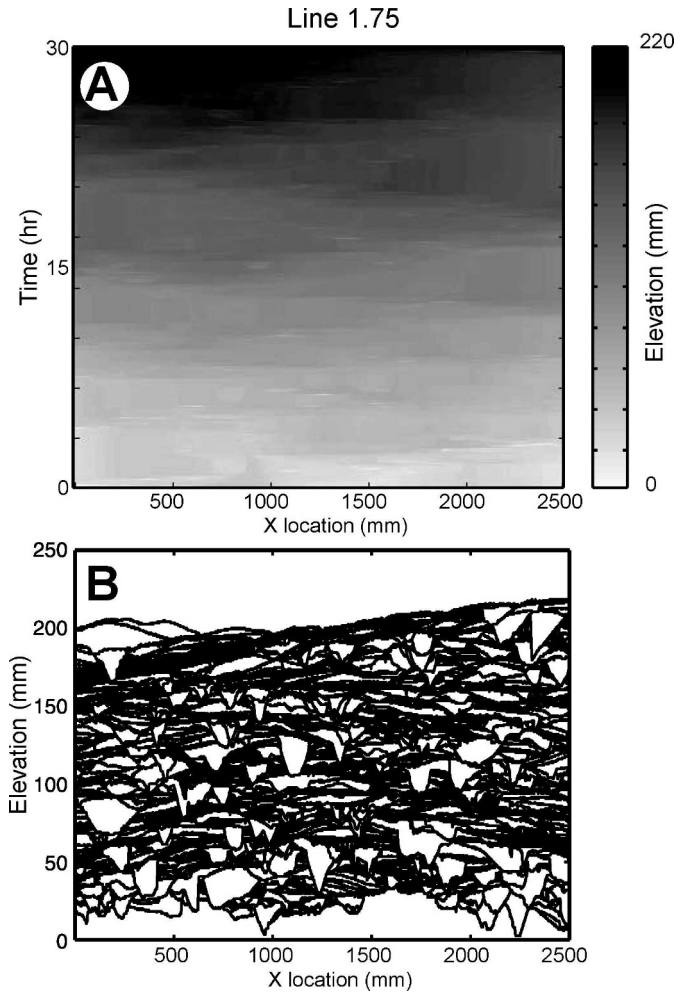

FIG. 8.— Data defining the evolution of topography during the DB03 experiment along a transect that is oriented approximately perpendicular to the dominant flow direction, 1.75 m from infeed point. **A)** Space time plot of sequential delta-top profiles shown every 120 s, with elevation represented by brightness. **B)** Synthetic stratigraphy generated through stacked delta-top profiles with topography clipped to account for sediment removed during erosional events. See Martin (2007) for explanation of clipping process.

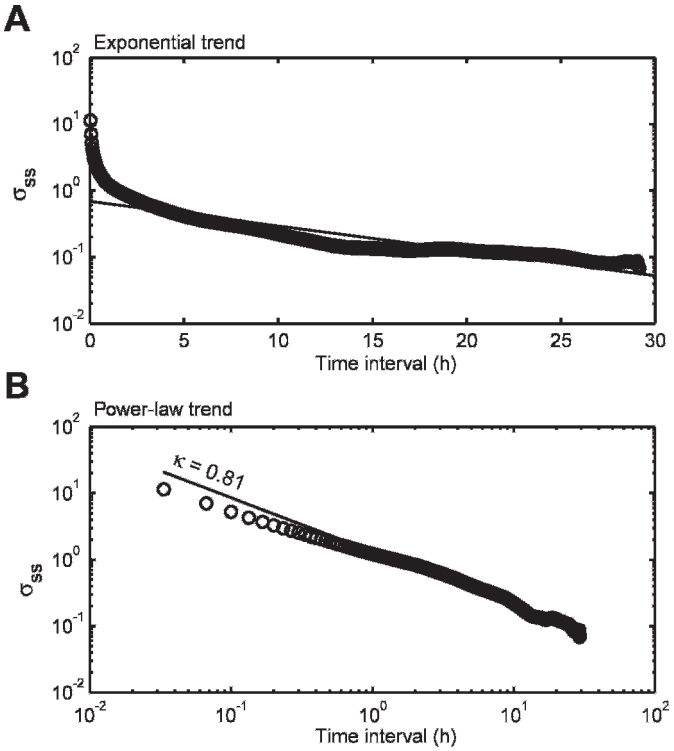

FIG. 9.— Decay of σ_{ss} with increasing time interval for the DB03 experiment. Data are fit with both **A)** exponential trend line and **B)** power-law trend line.

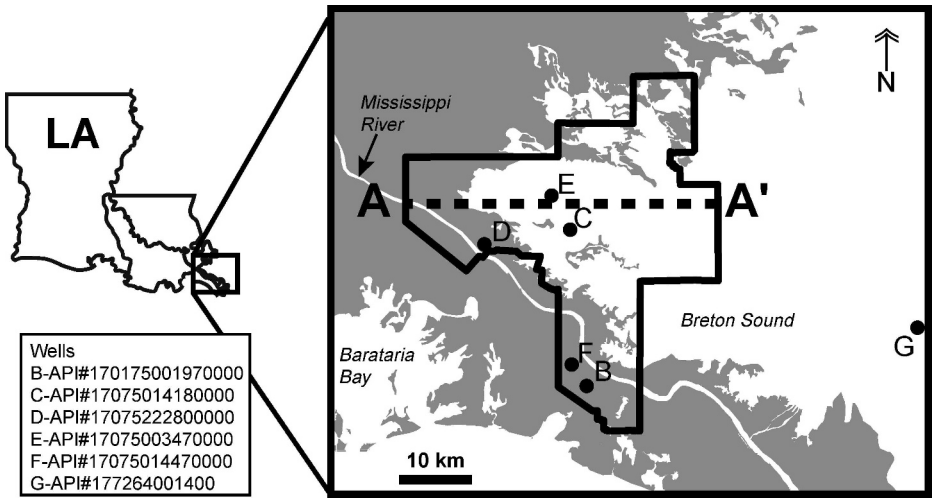

FIG. 10.—Location map of Breton Sound study region. Breton sound is situated about 100 km southwest of New Orleans, Louisiana in the Gulf of Mexico. Boundaries of industry-grade seismic are shown in thick black lines. Location of seismic section in Figure 13 is represented by dashed line. Location of wells utilized in time–depth algorithm and biostratigraphy are shown with black circles and labeled B–G.

The next step is to create maps of subsidence to complement maps of stratigraphic thickness. As was the case for the study of the Fisk basin stratigraphy, we lack a measure of subsidence in the Mississippi Delta independent from the sedimentation history. Further, we lack a high-resolution chronostratigraphic framework for this region of the Mississippi Delta. To counter these limitations, we have modified the methods of Lyons (2004) to measure the decay of σ_{ss} as a function of mean interval thickness rather than measurement time. We assume that our thickest stratigraphic interval (MD9–seafloor) is a reasonable approximation to basin subsidence at every grid location. Second, we assume that these local subsidence rates remained roughly constant over the time interval required to deposit the measured sections. These assumptions allow us to calculate a dimensional subsidence map for a stratigraphic interval with the equation

$$S_{Dim} = S_{Norm}\tilde{\partial}\eta_{-a-b} \tag{6}$$

where S_{Dim} is a matrix describing the dimensional subsidence as a function of position, S_{Norm} is a normalized subsidence matrix, and $\tilde{\partial}\eta_{-a-b}$ is the mean thickness of a stratigraphic unit bounded by seismic horizons *a* and *b*. With our above assumptions, we approximate S_{Norm} as the matrix of stratigraphic thickness for the interval bound by MD9 and the seafloor, divided by the maximum thickness value in that matrix (Fig. 15).

After maps of sedimentation and subsidence have been created we calculate maps of sedimentation/subsidence for all 44 stratigraphic intervals. Finally, the matrix of points defining a map of sedimentation/subsidence allows us to calculate σ_{ss} for each stratigraphic interval. Figure 16 displays the results of our analysis, with σ_{ss} plotted against mean stratigraphic unit thickness. We fitted the data with both

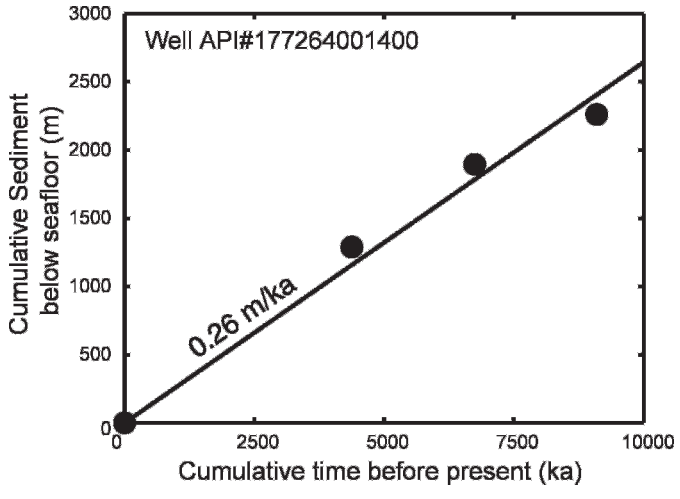

FIG. 11.—Age vs. sediment thickness below seafloor plot for Breton Sound. Age data were determined from calcareous nanofossil biostratigraphic markers identified in Well API# 177264001400 (identified as Well G in Figure 10). Sediment thickness was uncompacted to near-seafloor conditions. Best-fit trend line gives a long-term sedimentation (or subsidence) rate of 0.26 m/kyr with an R^2 value of 0.98.

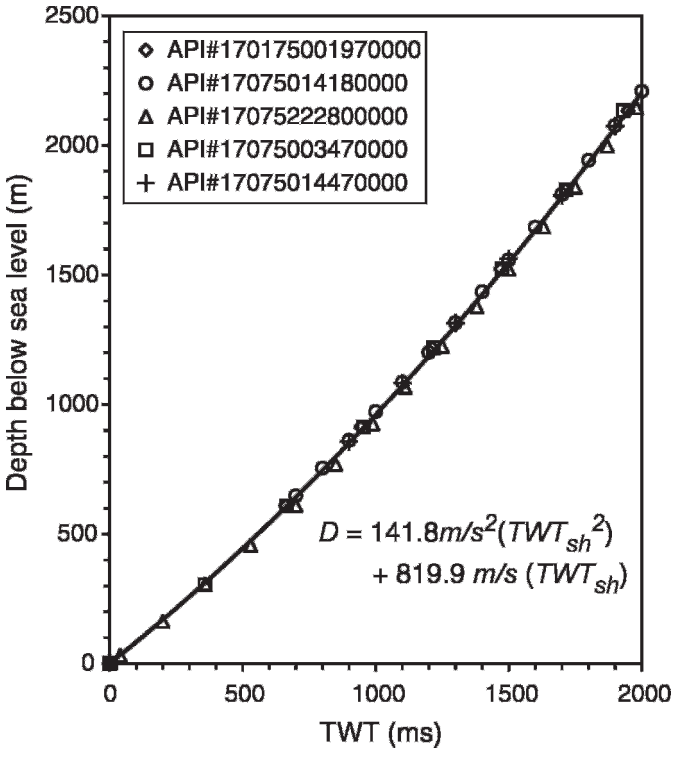

FIG. 12.—Time-depth relationship used to convert seismic data in TWT to true vertical depth. This relationship is derived from checkshot data from five well location within our study region and was applied basin-wide. Well locations are presented in Figure 10.

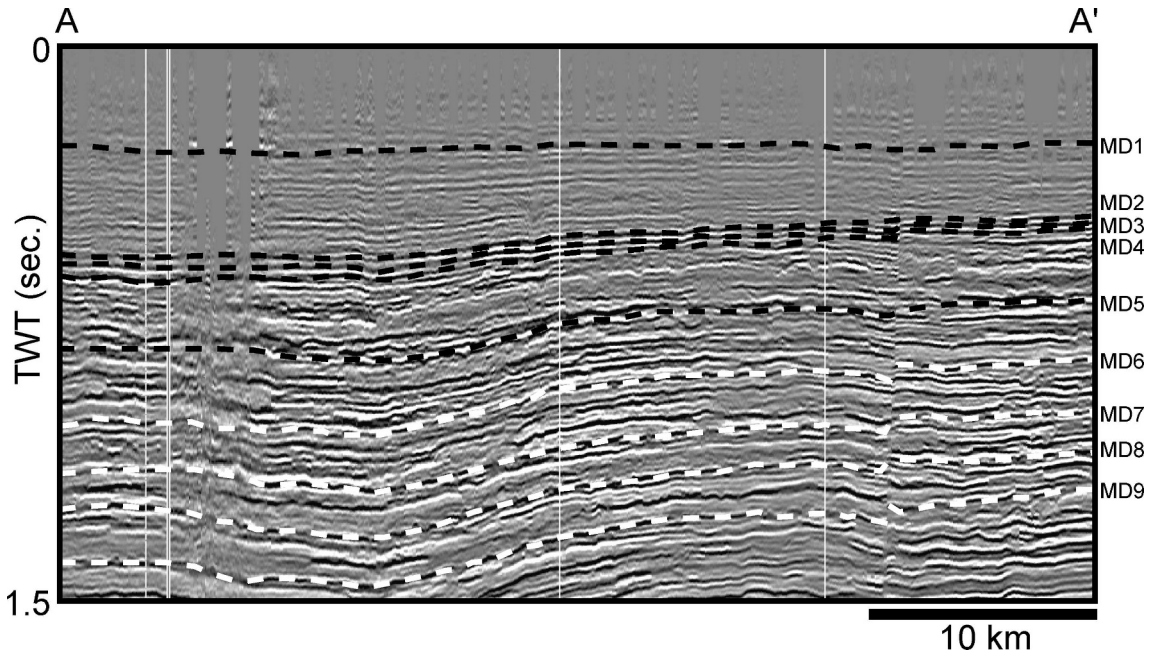

FIG. 13.—Characteristic strike-oriented seismic line for the study region. Dashed lines labeled MD1–MD9 follow mapped subsurface seismic horizons used in this study. Location of this seismic cross sections is marked in Figure 10.

exponential and power-law trends to estimate the stratigraphic integral scale and κ for this region of the Mississippi Delta. An exponential trend resulted in an R^2 value for the fit of 0.87. We can use the e-folding length from our fit to estimate a stratigraphic integral scale in vertical thickness of 556 m. Using our estimate of 0.26 m/kyr for the long-term subsidence rate in our study region, the stratigraphic integral scale in thickness equates to a stratigraphic integral scale in time units of 2.1 Myr. A power-law trend resulted in an R^2 of 0.94. This fit gives a κ value equal to 0.74.

A summary of the κ values found for all the studied experimental and field cases is presented in Table 1.

DISCUSSION

The term "compensational stacking" is used to describe the architecture of stratigraphy over a diverse range of depositional environments. For example, interpretations of channel and lobe deposits recorded in both deep marine and fluvial stratigraphy have used this concept. In the preceding sections we have developed the power-law decay rate κ of variability in local deposition rate with averaging interval σ_{ss} as a measure of the effectiveness of compensation during deposition. Is the decay rate κ for a particular basin strongly influenced by depositional environment? The magnitude of κ might be expected, for example, to vary between deep marine and fluvial settings as a result of differences in sediment transport processes. For example, the ratio of current density to ambient fluid density, ρ_c/ρ_a, for terrestrial fluvial systems is approximately 800 times greater than for submarine turbidity-current channel systems.

The value of ρ_c/ρ_a has been shown to influence the morphodynamics of channels in submarine and terrestrial environments (Imran et al. 1998). Of particular importance to this study, the value of ρ_c/ρ_a was shown to set the magnitude of channel superelevation (ratio of channel levee aggradation to flow depth) necessary to drive avulsions in the two settings (Mohrig et al. 2000). Mohrig et al. (2000) found that channel levees rarely aggrade more than 0.6 times channel depth before avulsing, while submarine superelevation can often exceed 1.5 (Pirmez and Flood 1995). Mohrig et al. suggested that this difference in superelevation probably results in reduced reoccupation of channels in submarine environments relative to terrestrial environments. A reduction in the reoccupation of previous submarine channels should therefore increase the value of κ in submarine relative to terrestrial basins. The values of κ measured in four experimental-basin scenarios and two field-scale basins ranged between 0.48 and 0.92. While the uncertainty of κ in these basins is substantial (Fig. 17) it is noteworthy that the highest κ value measured came from Fisk Basin, the only submarine basin in our study.

Stratigraphic Implications of κ

The range of measured κ values for the basins in our study points to the combined influence of compensation and stochastic processes in determining the architecture of sedimentary deposits. With the exception of Stage 3 of the XES-99 experiment, all measured values were between 0.5 (uncorrelated stacking) and 1.0 (pure compensational stacking). Given that the κ value of Stage 3 of the XES-99 experiment has greater uncertainty than any other data set we analyzed, we consider the measured value, 0.48, to be indistinguishable from the purely random stacking value of 0.5. Further, we believe that our high-temporal-resolution measurements from the DB-03 experiment support the construction of the compensation index using a power-law fit as opposed to the exponential fit employed by Sheets et al. (2002).

While the measured κ values are important for quantifying the degree of compensation in a basin, they are of little meaning for predicting the magnitude of σ_{ss} for a particular stratigraphic interval without knowledge of the leading coefficient, a, in the power-law fit presented in Equation 3. Confronted with a similar situation, Sheets et al. (2002) nondimensionalized their stratigraphic integral (time) scale by the amount of time necessary to aggrade a vertical distance equal to the mean channel depth. This normalization did an effective job of collapsing their observations. They found that regardless of the sedimentation and subsidence rates in their experiment the stratigraphic integral scale was equal to the time necessary to aggrade a thickness equal to about seven channel depths. Motivated by this finding, we have nondimensionalized the measurement windows associated with all values of σ_{ss} presented for the six analyzed systems by their associated estimated channel depths (Table 3). Rather

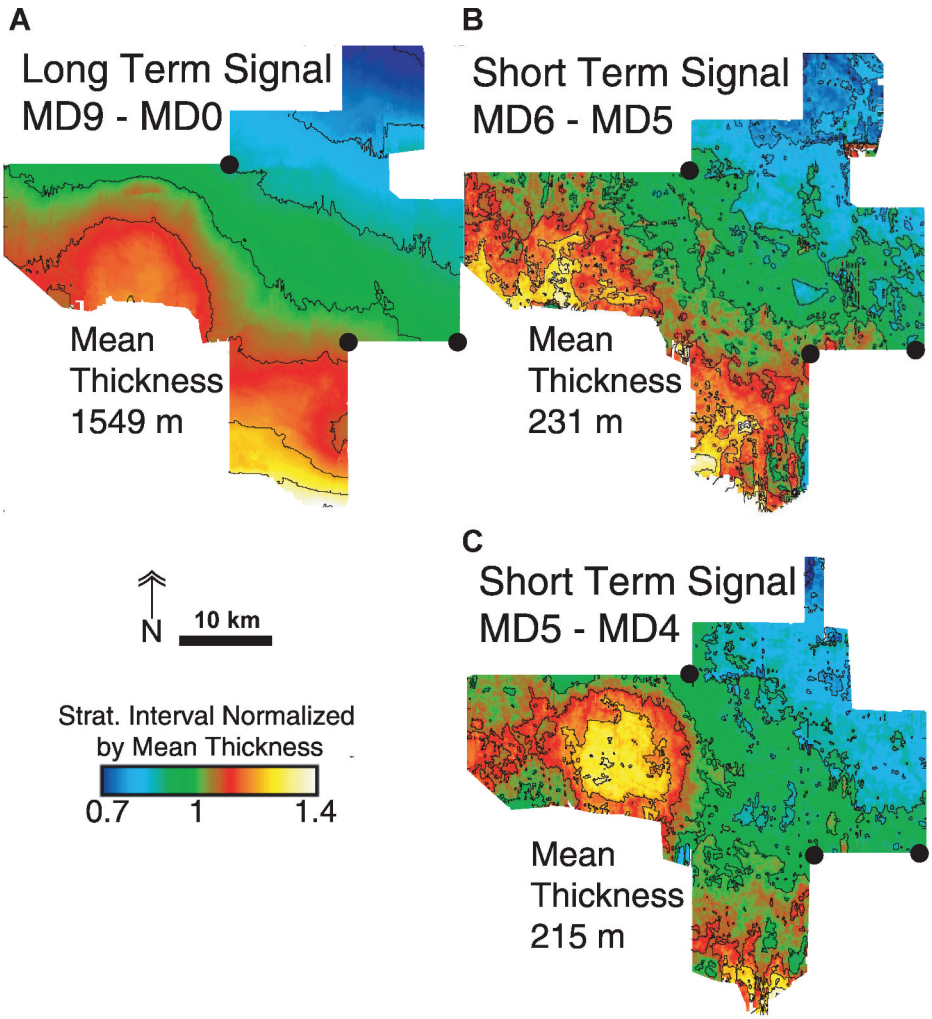

FIG. 14.—Maps of deposit thickness measured between regionally mapped seismic horizons. Maps are normalized by mean thickness of stratigraphic interval. **A)** Representative map of long-term deposition signal: deposit thickness of section between horizons MD9 and MD0 (present-day seafloor) with contour interval equal to 0.1 m/m. B, C) Representative maps of short-term deposition signal: **B)** thickness of deposit measured between horizons MD6 and MD5 with contour interval equal to 0.1 m/m; **C)** thickness of deposit measured between horizons MD5 and MD4 with contour interval equal to 0.1 m/m.

than converting thickness to time we instead used channel depth as a vertical reference scale (Fig. 18). This allows consideration of data sets that lack age control (e.g., the Mississippi Delta). Figure 18 shows that this normalization effectively collapses all of our σ_{ss} observations onto a single power-law trend with $\kappa \approx 0.75$. This finding suggests that on average, stratigraphy of sedimentary basins is constructed with architecture roughly half-way between purely compensational and purely random. We stress that this finding does not imply that all basins have $\kappa = 0.75$. Rather, we predict that for most basins κ will range between 0.5 and 1 depending on local transport processes, as is seen in the data sets analyzed in this manuscript. Cases with significant depositional persistence could produce $\kappa < 0.5$, but none of the data sets we analyzed show this within measurement uncertainty. However, the data suggest that $\kappa \approx 0.75$ represents the global average architecture of channel-associated strata, and thus provides an initial reference value for modeling and prediction.

The collapse of data defining the decay of σ_{ss} as a function of aggradation thickness/channel depth has several implications for the interpretation of stratigraphy. First, regardless of depositional environment, the dominant vertical scale controlling stratigraphic architecture in channelized systems is channel depth. Other variables describing

→

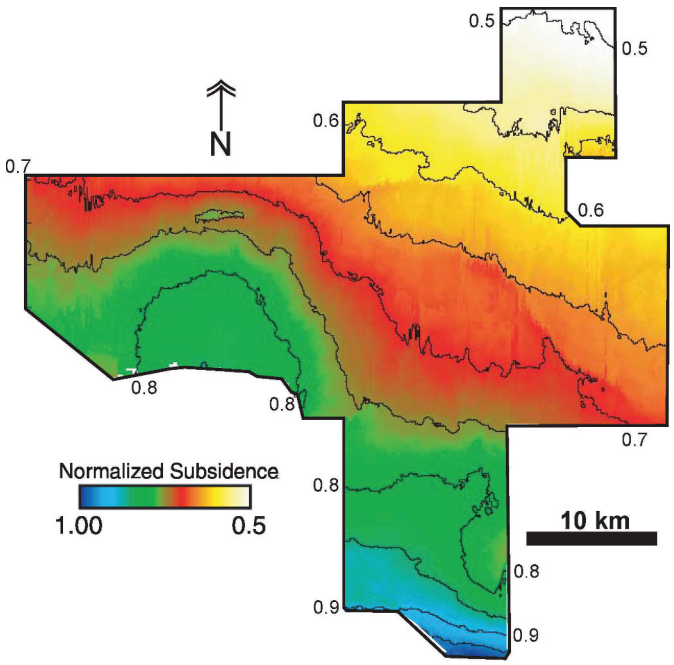

FIG. 15.— Normalized subsidence map for Breton Sound study region. Map created by point wise division of isopach map MD9–MD0 by maximum thickness for this interval map. Contour interval is equal to 0.05 m/m.

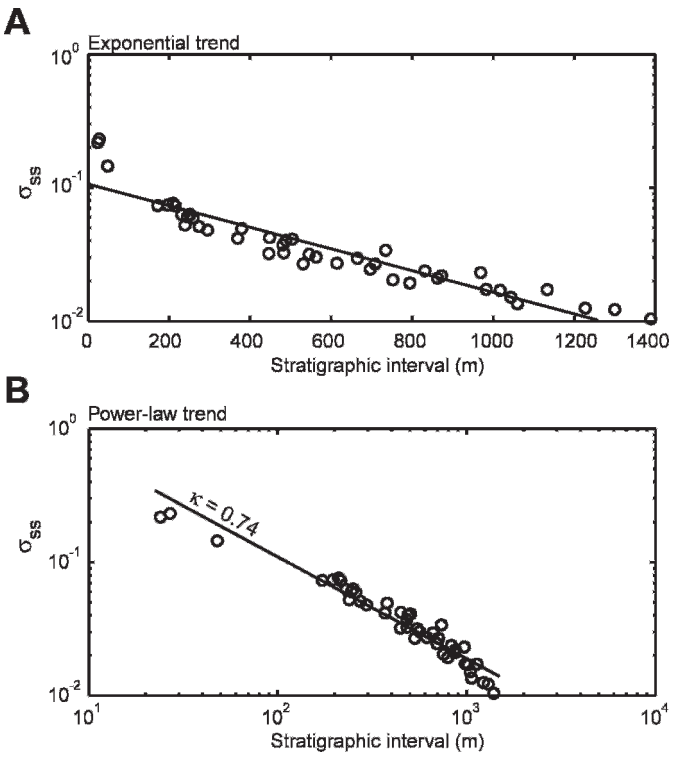

FIG. 16.—Decay of σ_{ss} with increasing time interval for the Mississippi Delta in the Breton Sound study region. Data are fitted with both **A)** exponential trend line and **B)** power-law trend line.

depositional environment play important roles in the structure of preserved depositional elements, but the stacking of these elements is to first order controlled by channel depth. This is highlighted by the fact that our analysis includes experimental-scale and field-scale basins, with characteristic channel depth scales ranging from 0.01 m to 50 m, in addition to fluvial and deep-water basins.

While the specific value of the compensation index, κ, varies between 0.48 to 0.92 for the six data sets in our study, the value of the nondimensional power law constant, a, is remarkably similar for all data sets. Equation 3 can be rearranged to solve for a with T replaced by our nondimensionalized aggradation $\left(\frac{d\eta}{H_C}\right)$:

$$a = \frac{\sigma_{ss}}{\left(\frac{d\eta}{H_C}\right)^{-\kappa}} \tag{7}$$

where H_C is the mean channel depth in the basin. After nondimensionalization using average channel depths, the mean value of a over our six data sets is 0.33, with an associated standard deviation of 0.07. Rearranging Equation 7 results in $H_c/d\eta = 1$ for the case of $\sigma_{ss} = 0.33$ since $a = 0.33$. Thus across the six study cases, we have overall:

$$H_C = d\eta|_{\sigma_{SS}=0.33} \tag{8}$$

Equation 8 can be used to provide an initial estimate of the mean depth of channels responsible for the construction of a stratigraphic section if the $d\eta$ associated with a σ_{ss} equal to 0.33 is known, or vice versa.

Parameters Controlling κ

Our measurements of κ suggest that pooling all the basins we studied, stratigraphic architecture falls roughly midway between fully compensational stacking and uncorrelated random stacking. What are the possible scenarios that could result in κ values in this range? We explore this question using a sequence of quantitative thought experiments in which we fill a model 2D basin with discrete depositional elements. We use only one element shape, a triangle that we deposit in the basin at every time step. The triangular deposits are meant to represent either channel or fan deposits that have maximum thickness near their centerline and thin moving laterally away from the centerline. During each model time step we deposit one element in the basin. Subsidence is set to balance mean aggradation in the basin for each time step. To study the scenarios that lead to different values of κ we alter both the size of the depositional element at every time step and the lateral position of a deposit relative to

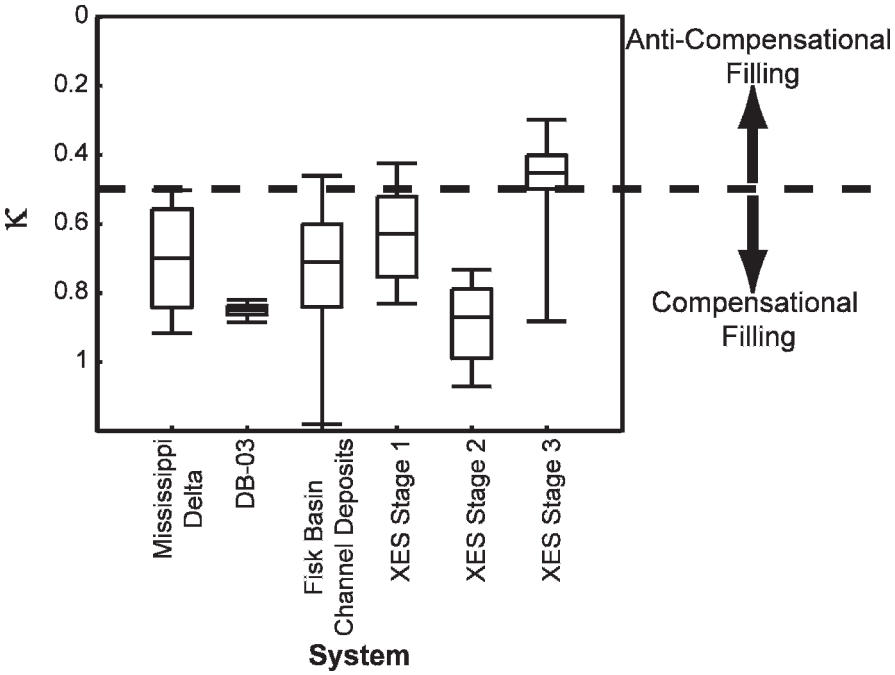

FIG. 17.—Box and whisker plots to compare mean κ values and associated errors of six data sets in this study. Mean κ and associated errors of each data set were determined by bootstrapping analysis. Boundaries of boxes represent 75th percentile confidence levels. Whiskers represent 95th percentile confidence levels.

TABLE 3.—*Mean channel depths of six data sets in this study.*

System	Mean Channel Depth (m)
XES99 - Stage 1[1]	1.8×10^{-2}
XES99 - Stage 2[1]	1.9×10^{-2}
XES99 - Stage 3[1]	1.5×10^{-2}
DB-03	1.8×10^{-2}
Fisk Basin[2]	50
Breton Sound[3]	25

[1] (Sheets et al. 2002), [2] (Lyons 2004), [3] (Coleman et al. 1998).

both the location of deposition at the previous time step and the locations of topographic minima.

We start by analyzing the difference between a model (S1) in which a deposit is placed at the absolute topographic low during each time step (maximum compensation) and a model (S2) in which a deposit is placed at a randomly assigned location during each time step (no compensation). The stratigraphy resulting from each scenario is shown in Figure 19. With this stratigraphy and our imposed model subsidence we calculate the σ_{ss} for every possible measurement window and use this data to measure κ. We find, not surprisingly, that for the first scenario $\kappa = 1.0$ (pure compensation) and for the second scenario $\kappa = 0.5$ (no compensation).

To analyze the effect of scale in these numerical experiments we ran several versions of scenarios S1 and S2 where we varied the size of the depositional element relative to the size of the model domain. We found that as long as the depositional element is no more than half as large as the model domain, the resulting value of κ was unaffected by changes in relative element size.

The first two scenarios are associated with transport systems that are free to avulse to any location in a basin at every time step. However, we know that on short time scales the probability of an avulsion is low. As such, we next calculate κ under two scenarios where the position of depositional elements can migrate laterally only by a length that is less than the width of deposition during any one time step. The two scenarios are: (1) the locus of deposition follows a random walk and deposition randomly migrates either to the left or right of the center position of the deposit at the previous time step by one element width (S3); and (2) a depositional element is placed in the lowest position that is within one element width either left or right of the location of deposition in the previous time step (S4). We find that the former scenario (S3) leads to a κ value of 0.3, i.e., it is anti-compensational, while the latter scenario (S4) once again results in a κ value of 1.0. While the systems that we have analyzed are primarily compensational on the time scales we analyze, there is good evidence that some systems are anti-compensational on short time scales. For example recent field studies and numerical models have shown that abandoned river channels serve as attractors until they are filled with sediment, leading to development of multistory channel bodies and channel deposit clusters (Hajek et al. 2006; Jerolmack and Paola 2007; Mohrig et al. 2000). Whenever a depositional element acts as an attractor, it tends to create persistence and anti-compensation. In contrast, compensation is essentially the result of depositional elements acting as local repellers.

None of the scenarios presented thus far results in a κ value near our measured overall value of 0.75. This is because we constructed the scenarios to be controlled entirely by either compensation or by purely random processes. Next, we analyze a scenario that shares characteristics of both compensation and random processes. In this scenario (S5) we combine attributes of scenarios S1 and S3. With some pre-selected integer n, for $n - 1$ time steps the system follows the rules set for S3, random migration of the locus of deposition to either the left or right by less than one deposit width. However, at every nth time-step the center of deposition relocates to the absolute topographic low in the model

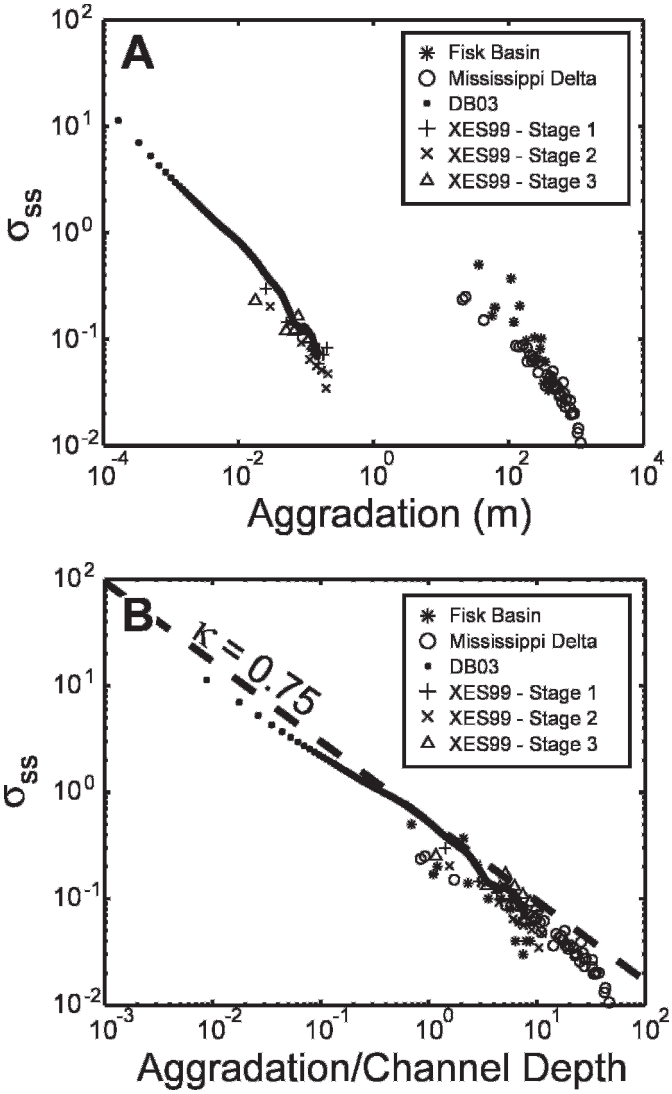

FIG. 18.—Collapse of decay of σ_{ss} for data sets in this study. **A)** Decay of σ_{ss} for six data sets in this study prior to nondimensionalization. **B)** Decay of σ_{ss} plotted against nondimensionalized aggradation for six data sets in this study. For each data set, measurement window was nondimensionalized by mean depth of system. Thick gray dashed line represents decay trend with $\kappa = 0.75$.

domain, i.e., it behaves compensationally (Fig. 20A, B). For the size of our model domain and $n = 20$, the combination of these two processes results in a κ values equal to 0.75. We have found that for a given avulsion frequency κ is sensitive to the ratio of the size of the depositional element to the size of the model domain undergoing subsidence. However, for any given ratio of model domain size to depositional element size, κ values increase logarithmically as the frequency of system-scale avulsions increases. Hence, by varying the relative size of the avulsing element and the avulsion frequency, one can produce the full range of values between 0.5 and 1.0.

Finally, there is a second way of producing κ values between 0.5 and 1.0 that does not require intermittent avulsions to topographic minima superimposed on stochastic migration of the locus of deposition. This final scenario (S6) was motivated by observations of sediment storage and release events from experiments in subsiding basins (Kim et al. 2006) and numerical channel avulsion models (Jerolmack and Paola 2007). These studies found that time series of sediment discharge can fluctuate even in

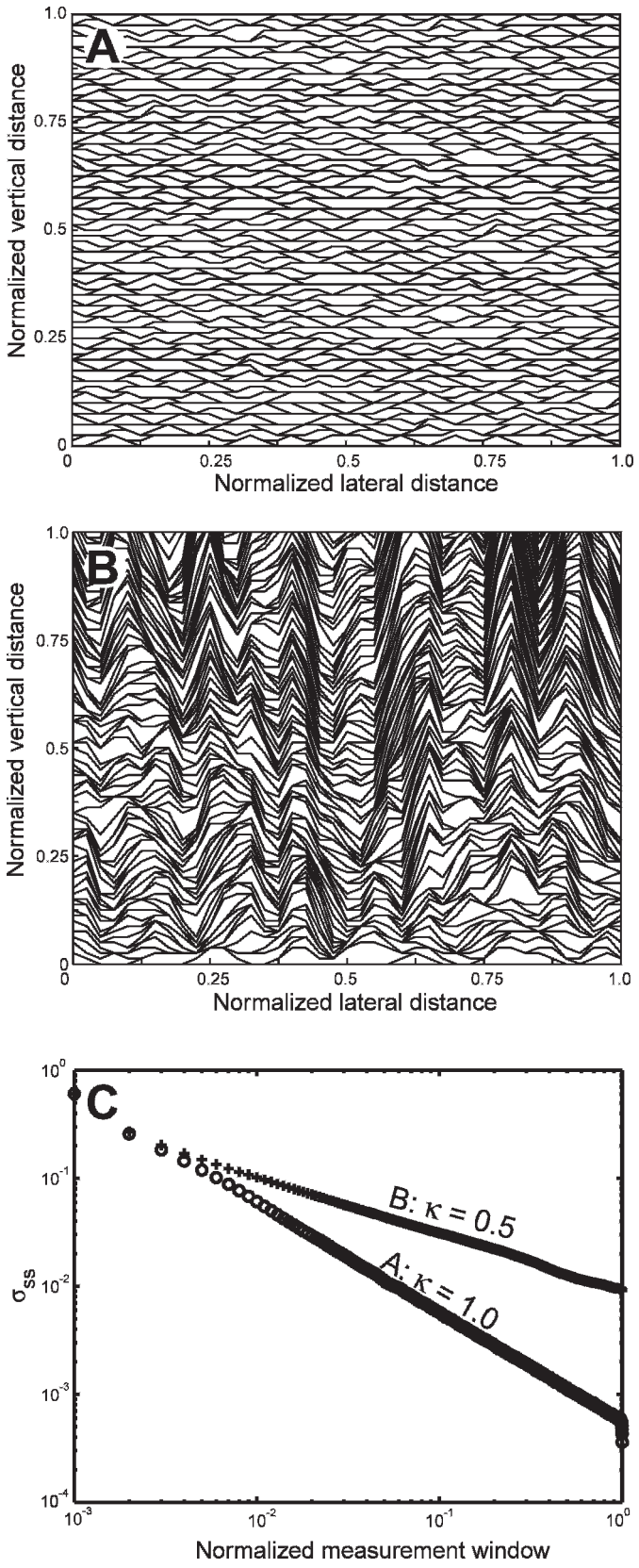

FIG. 19.—Comparison of results from 2D stratigraphic architecture models. **A)** We present the stratigraphy created by model S1. In this model symmetrical triangular deposits are placed in the absolute topographic low during each time step. **B)** We present the stratigraphy created by model S2. In this model symmetrical triangular deposits are placed in a random lateral location within the model domain during each time step. Time lines associated with every tenth model time-step are displayed in Parts A and B. The size of triangular deposits associated with each time-step is the same for Parts A and B. In Part C we present the decay of σ_{ss} with measurement window for both scenarios. We find that model S1 is associated with a κ value of 1.0 while model S2 is associated with a κ value of 0.5.

basins that are experiencing constant boundary conditions due to autogenic sediment storage and release events. To incorporate this effect, we construct a scenario similar to S4, migration of the locus of deposition during every time step to the lowest topographic spot within one deposit width of the locus of deposition from the previous time step. In addition, though, the magnitude of deposit thickness in this scenario was randomly assigned from a Gaussian distribution during each time step. The combination of local compensational stacking and unsteadiness in deposition rates leads again to κ values between 0.5 and 1.0 (Fig. 20C, D). In this case, κ is controlled by the variability of deposition rate: as the standard deviation of the Gaussian distribution of deposit thicknesses decreases, the system κ values increase linearly.

All of the simple models explored above implicitly assume constant external conditions. However, it is well documented that changes in boundary conditions (allogenic forcings) can also cause short-term variability in sediment transport rates in sedimentary basins. Examples of this include sequence stratigraphic models where changes in climate or base level influence volumes of sediment stored in terrestrial and marine environments (Perlmutter et al. 1995; van Wagoner 1995). We expect that κ is influenced by allogenic variability in sediment transport rates, but it is difficult at present to separate the signal of this variability from autogenic variability. To illustrate this point we note the similar κ values of the DB03 experimental stratigraphy and the Breton Sound stratigraphy. The DB03 experimental stratigraphy experienced constant subsidence rates and input water and sediment discharges while the section of the stratigraphy analyzed in the Breton Sound data set was deposited over a time period when sea level varied over several glacial cycles (Salvador 1991). Analyzing changes in compensation index with allogenic forcing would be a valuable next step in understanding the connection between autogenic and allogenic processes in stratigraphy.

Compensation and the Sadler Effect

Deposition events create deposits with a wide range of thicknesses, but as strata accumulate over the course of many deposition and erosion events, extreme events are preferentially preserved in the sedimentary record. Sadler (1981) noted that this incompleteness of the sedimentary record results in a systematic decay of deposition rates with increasing time (i.e., thickness) interval of measurement. Because extreme events are preferentially preserved, bed thicknesses tend to correspond with extreme deposition rates, i.e., several standard deviations above the mean. Indeed, using a much larger dataset, Strauss and Sadler (1989) showed that the standard deviation of deposition rate in random-walk deposition models (such as discussed in Section 3) predicts the power-law decay in time-averaged deposition rates observed in diverse depositional environments. Our compensation index κ can be converted directly to an exponent of the form developed by Jerolmack and Sadler (2007). They find that an exponent equivalent to $\kappa \approx 0.75$, corresponding to noisy diffusion, describes decay in deposition rates well across a wide range of depositional environments. This is consistent with our aggregate dataset (Fig. 18), which also gives an overall power law with $\kappa \approx 0.75$. Additionally, the data in Jerolmack and Sadler (2007) suggest weaker compensation in shelf and floodplain environments, where transport is

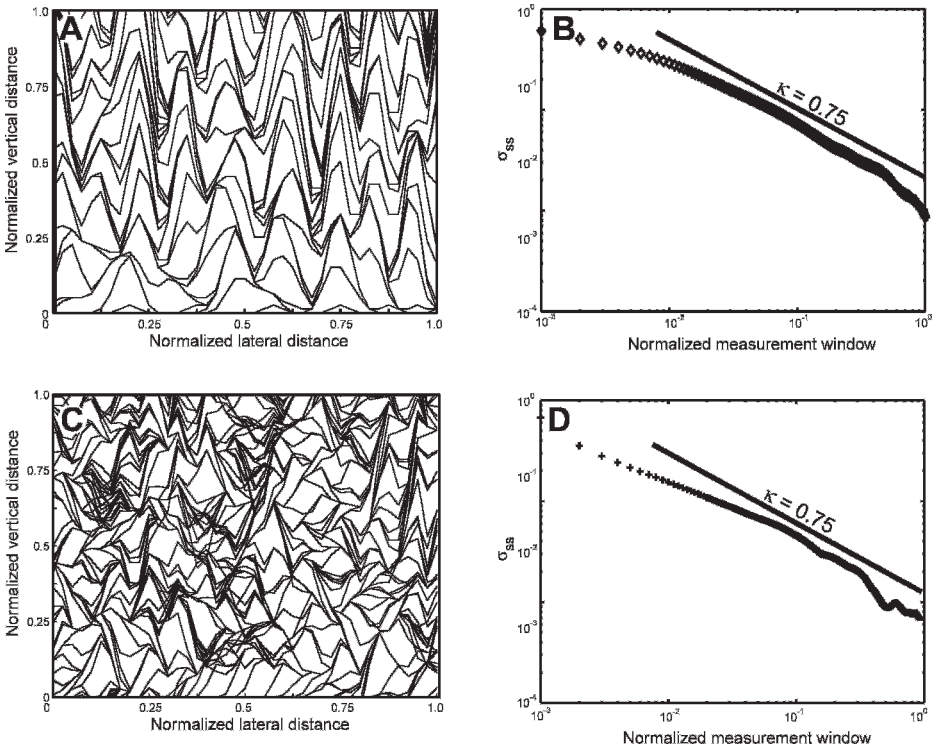

FIG. 20.—Comparison of results from 2D stratigraphic architecture models. **A**, **B)** We present results from stratigraphy created by model S5. In this scenario, during the majority of time steps symmetrical triangular deposits are randomly placed one deposit width either to the left or to the right of the site of deposition from the previous time step. However, during every twentieth time step the site of deposition migrates to the absolute topographic low. Time lines associated with every tenth model time step are shown in Part A and the decay of σ_{ss} with measurement window is shown in Part B. Deposit size and shape are the same as those associated with models S1 and S2 (Fig. 19). **C**, **D)** We present results from stratigraphy created by model S6. In this scenario, symmetrical triangular deposits are placed in the absolute topographic low during each time step. The size of the deposit at each time step is randomly assigned from a Gaussian distribution of sizes that has a mean equal to the deposit size from models S1, S2, and S5 with a standard deviation equal to 1.50 (mean deposit size). Time lines associated with every tenth model time step are shown in Part C, and the decay of σ_{ss} with measurement window is shown in Part D.

less strongly slope-driven (e.g., sediment delivered by waves or widespread inundation), giving $\kappa \approx 0.52$ to 0.56. This is consistent with our finding that κ is highest (most compensational) in deep-water, lobe-dominated settings.

Implications for Reservoir Modeling

Our analysis of six sedimentary systems suggests that κ can span the full range from 0.5 to 1.0 but on average resides mid-way between these two extremes. This finding can be applied directly to geostatistical reservoir models that use compensational stacking routines to fill model space. For example the stochastic surface-based model of turbidite lobes developed by Pyrcz et al. (2005) uses algorithms to place architectural elements within a model domain. The placement of these elements results in perfect compensational stacking of turbidite lobes ($\kappa = 1$). Our findings suggest that, while possible, this represents an end-member scenario. In the absence of a better understanding of controls on κ, we suggest using a range of simulation scenarios that give a range of κ values, including the observed overall average case of $\kappa = 0.75$.

CONCLUSIONS

1. We have developed and implemented a method for quantifying compensational stacking in sedimentary basins. This method uses the decay of the standard deviation of the ratio of sedimentation to subsidence σ_{ss} with increasing measurement window. The decay of σ_{ss} follows a power law, and we term the power-law exponent the *compensation index*, κ. For pure compensational stacking, i.e., deposition always fills topographic lows, $\kappa = 1.0$. Where stacking is random, uninfluenced by topography, $\kappa = 0.5$. In the limit of pure anti-compensation (i.e., depositional persistence, in which low areas become lower), $\kappa = 0$.
2. Measurements from six experimental and field cases, including terrestrial and deep-water examples, show that most deposits fall in the range $0.5 < \kappa < 1.0$, i.e., partial compensation. When the aggradation of these systems is normalized by basin channel depth, the decay of σ_{ss} of these six systems collapses approximately onto a single power-law trend with $\kappa \approx 0.75$, midway between purely random and perfect compensation. Channel depth thus acts as a fundamental length scale controlling stratigraphic architecture across environments. This overall κ value can be used to provide an initial estimate of the magnitude of σ_{ss} for any stratigraphic window in which the mean channel depth is known, or vice versa.
3. Simple depositional models suggest that, even without external influences, the value of κ can be set by the frequency of channel avulsions in a basin, the size of depositional units relative to the basin, and the magnitude of sediment storage and release events in the basin.

NOTATIONS

A	area
a	power-law constant
D	depth below seafloor
φ	spatial correlation constant
H	sediment Thickness
H_c	channel Height
$d\eta$	bed thickness
κ	compensation index
r	sedimentation rate
ρ_a	ambient fluid density
ρ_c	current density
S	subsidence
σ_{ss}	standard deviation of sedimentation/subsidence
T	stratigraphic time
TWT	two-way travel time
x	horizontal location
y	horizontal location

ACKNOWLEDGMENTS

Support for our research was provided by the St. Anthony Falls Laboratory Industrial Consortium (ExxonMobil, ConocoPhillips, Japan National Oil Company, Shell, Chevron) and by the Science and Technology Center Program of the National Science Foundation via the National Center for Earth-Surface Dynamics under agreement EAR-0120914. Doug Jerolmack, Liz Hajek, and Vamsi Ganti are thanked for stimulating discussions that motivated and clarified several ideas in this manuscript. Morgan Sullivan, Mike Leeder, and Michael Pyrcz are thanked for constructive reviews which greatly improved this manuscript. Additionally, we thank WesternGeco for permission to publish seismic data from the Mississippi Delta.

REFERENCES

Allen, J.R.L., 1979, Studies in fluviatile sedimentation: an elementary geometrical model for the connectedness of avulsion-related channel sand bodies: Sedimentary Geology, v. 24, p. 253–267.

Anderson, J.B., Rodriguez, A., Abdulah, K., Fillon, R.H., Banfield, L.A., McKeown, H.A., and Wellner, J.S., 2004, Late Quaternary stratigraphic evolution of the Northern Gulf of Mexico Margin: A synthesis, *in* Anderson, J.B., and Fillon, R.H., eds., Late Quaternary Stratigraphic Evolution of the Northern Gulf of Mexico Margin: SEPM, Special Publication 79, p. 1–23.

Coleman, J.M., Roberts, H.H., and Stone, G.W., 1998, Mississippi River delta: An overview: Journal of Coastal Research, v. 13, p. 689–716.

Deptuck, M.E., Piper, D.J.W., Savoye, B., and Gervais, A., 2008, Dimensions and architecture of late Pleistocene submarine lobes off the northern margin of East Corsica: Sedimentology, v. 55, p. 869–898.

Fillon, R.H., Kohl, B., and Roberts, H.H., 2004, Late Quaternary deposition and paleobathymetry at the shelf–slope transition, ancestral Mobile River Delta Complex, Northeastern Gulf of Mexico, *in* Anderson, J.B., and Fillon, R.H., eds., Late Quaternary Stratigraphic Evolution of the Northern Gulf of Mexico Margin: SEPM, Special Publication 79, p. 111–141.

Galloway, W.E., and Hobday, 1996. Terrigenous Clastic Depositional Systems: New York, Springer, 489 p.

Galloway, W.E., Ganey-Curry, P.E., Li, X., and Buffler, R.T., 2000, Cenozoic depositional history of the Gulf of Mexico basin: American Association of Petroleum Geologists, Bulletin, v. 84, p. 1743–1774.

Hajek, E., Heller, P., Huzurbazar, S., Sheets, B., and Paola, C., 2006, Avulsion clusters in alluvial systems: An example of large-scale self-organization in ancient and experimental basins: EOS, Transactions, American Geophysical Union, v. 87, p. NG53A-03.

Hodgson, D.M., Flint, S., Hodgetts, D., Drinkwater, N.J., Johannessen, E.P., and Luthi, S.M., 2006, Stratigraphic evolution of fine-grained submarine fan systems, Tanqua Depocenter, Karoo Basin, South Africa: Journal of Sedimentary Research, v. 76, p. 20–40.

Imran, J., Parker, G., and Katopodes, N., 1998, A numerical model of channel inception on submarine fans: Journal of Geophysical Research, v. 103, p. 1219–1238.

Jerolmack, D.J., and Paola, C., 2007, Complexity in a cellular model of river avulsion: Geomorphology, v. 91, p. 259–270.

Jerolmack, D.J., and Sadler, P., 2007, Transience and persistence in the depositional record of continental margins: Journal of Geophysical Research, v. 112, F03S13, doi:10.1029/2006JF000555.

Johnson, S.D., Flint, S., Hinds, D., and De Ville Wickens, H., 2001, Anatomy, geometry and sequence stratigraphy of basin floor to slope turbidite systems, Tanqua Karoo, South Africa: Sedimentology, v. 48, p. 987–1023.

Kim, W., Paola, C., Swenson, J.B., and Voller, V.R., 2006, Shoreline response to autogenic processes of sediment storage and release in the fluvial system: Journal of Geophysical Research, v. 111, F04013, doi:10.1029/2006JF000470.

Leeder, M.R., 1978, A quantitative stratigraphic model for alluvium, with special reference to channel deposit density and interconnectedness, *in* Miall, A.D., ed., Fluvial Sedimentology: p. 587–596.

Lyons, W.J., 2004, Quantifying channelized submarine depositional systems from bed to basin scale [unpublished Ph.D. thesis]: Woods Hole Oceanographic Institution and Massachusetts Institute of Technology, Woods Hole, Massachusetts, 252 p.

Martin, J.M., 2007, Quantitative sequence stratigraphy [unpublished Ph.D. thesis]: University of Minnesota, Minneapolis, Minnesota, 193 p.

Mitchum, R.M., and Van Wagoner, J.C., 1991, High-frequency sequences and their stacking patterns: sequence-stratigraphic evidence of high-frequency eustatic cycles: Sedimentary Geology, v. 70, p. 131–160.

Mohrig, D., Heller, P.L., Paola, C., and Lyons, W.J., 2000, Interpreting avulsion process from ancient alluvial sequences: Guadalupe–Matarranya (northern Spain) and Wasatch Formation (western Colorado): Geological Society of America, Bulletin, v. 112, p. 1787–1803.

Morton, R.A., Tiling, G., and Ferina, N.F., 2003, Causes of hot-spot wetland loss in the Mississippi delta plain: Environmental Geosciences, v. 10, p. 71–80.

Mutti, E., and Sonnino, M., 1981, Compensational cycles: A diagnostic feature of turbidite sandstone lobes (abstract): International Association of Sedimentologists, Second European Regional Meeting, p. 120–123.

Mutti, E., and Normark, W.R., 1987, Comparing examples of modern and ancient turbidite systems: Problems and concepts, *in* Leggett, J.K., and Zuffa, G.G., eds., Marine Clastic Sedimentology: Concepts and Case Studies: Boston, Graham and Trotman, p. 1–38.

Olariu, C., and Bhattacharya, J.P., 2006, Terminal distributary channels and delta front architecture of river-dominated delta systems: Journal of Sedimentary Research, v. 76, p. 212–233.

Paola, C., Mullin, J., Ellis, C., Mohrig, D., Swenson, J.B., Parker, G., Hickson, T., Heller, P.L., Pratson, L., Syvitski, J.P.M., Sheets, B., and Strong, N., 2001, Experimental Stratigraphy: GSA Today, v. 11, p. 4–9.

Pelletier, J.D., and Turcotte, D.L., 1997, Synthetic stratigraphy with a stochastic diffusion model of fluvial sedimentation: Journal of Sedimentary Research, v. 67, p. 1060–1067.

Perlmutter, M.A., Radovich, B.J., Matthews, M.D., and Kendall, C.G.S.C., 1995, The impact of high-frequency sedimentation cycles on stratigraphic interpretation, *in* Gradstein, F.M., Sandvik, K.O., and Milton, N.J., eds., Sequence Stratigraphy: Concepts and Applications, Norwegian Petroleum Society, Special Publication 8, p. 141–170.

Pirmez, C., and Flood, R.D., 1995, Morphology and structure of Amazon channel, *in* Flood, R.D., Piper, D.J.W., Klaus, A., and Peterson, L.C., eds., Proceedings of the Ocean Drilling Program, Initial Results: College Station, Texas, Ocean Drilling Program, p. 23–45.

Pyrcz, M.J., Catuneanu, O., and Deutsch, C.V., 2005, Stochastic surface-based modeling of turbidite lobes: American Association of Petroleum Geologists, Bulletin, v. 89, p. 177–191.

Raymer, L.L., Hunt, E.R., and Gardner, J.S., 1980, An improved sonic transit time-to-porosity transform: The Society of Petrophysicists and Well Log Analysts, Annual Logging Symposium: p. P1–P13.

Sadler, P., 1981, Sediment accumulation and the completeness of stratigraphic sections: Journal of Geology, v. 89, p. 569–584.

Salvador, 1991, Origin and development of the Gulf of Mexico basin, *in* Salvador, A., ed., The Gulf of Mexico Basin, Volume J: The Geology of North America: Geological Society of America, p. 131–180.

Satur, N., Hurst, A., Cronin, B.T., Kelling, G., and Gurbuz, K., 2000, Sand body geometry in a sand-rich, deep-water clastic system, Miocene Cingoz Formation of southern Turkey: Marine and Petroleum Geology, v. 17, p. 239–252.

Schuster, D.C., 1995, Deformation of allochthonous salt and evolution of related salt-structural systems, Eastern Louisiana Gulf Coast, *in* Jackson, M.P.A., Roberts, D.G., and Nelson, S., eds., Salt Tectonics: A Global Perspective: American Association of Petroleum Geologists, p. 177–198.

Sheets, B., Hickson, T.A., and Paola, C., 2002, Assembling the stratigraphic record: depositional patterns and time-scales in an experimental alluvial basin: Basin Research, v. 14, p. 287–301.

Sheets, B.A., Paola, C., and Kelberer, J.M., 2007, Creation and preservation of channel-form sand bodies in an experimental alluvial system, *in* Nichols, G., Williams, E., and Paola, C., eds., Sedimentary Processes, Environments and Basins: Oxford U.K., Blackwell Publishing, 648 p.

Stow, D.A.V., and Johansson, M., 2000, Deep-water massive sands: nature, origin and hydrocarbon implications: Marine and Petroleum Geology, v. 17, p. 145–174.

Strauss, D.J., and Sadler, P., 1989, Stochastic models for the completeness of stratigraphic sections: Mathematical Geology, v. 21, p. 37–59.

Van Beek, J.L., and Meyer-Arendt, K.J., 1982. Louisiana's eroding coastline: Recommendations for protection: Baton Rouge, Louisiana Department of Natural Resources.

van Wagoner, J.C., 1995, Sequence stratigraphy and marine to non-marine facies architecture of foreland basin strata, Book Cliffs, Utah, U.S.A., *in* van Wagoner, J.C., and Bertram, G.T., eds., Sequence Stratigraphy of Foreland Basin Deposits: Outcrop and Subsurface Examples from the Cretaceous of North America: American Association of Petroleum Geologists, p. 137–223.

Weimer, P., 1990, Sequence stratigraphy, facies geometries, and depositional history of the Mississippi Fan, Gulf of Mexico: American Association of Petroleum Geologists, Bulletin, v. 74, p. 425–453.

Winker, C.D., and Booth, J.R., 2000, Sedimentary dynamics of the salt-dominated continental slope, Gulf of Mexico: Integration of observations from the seafloor, near-surface, and deep subsurface: SEPM, Gulf Coast Section, 20th Annual Research Conference: Deep-Water Reservoirs of the World, p. 1059–1086.

Received 26 September 2008; accepted 30 March 2009.